NASA/TM-2005-213525

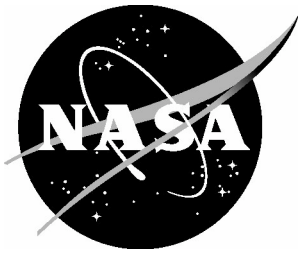

X-43A Rudder Spindle Fatigue Life Estimate and Testing

Edward H. Glaessgen
Langley Research Center, Hampton, Virginia

David S. Dawicke
Analytical Services and Materials, Inc.
Langley Research Center, Hampton, Virginia

William M. Johnston
Lockheed Martin Engineering and Sciences
Langley Research Center, Hampton, Virginia

Mark A. James
National Institute of Aerospace
Langley Research Center, Hampton, Virginia

Micah Simonsen
Correlated Solutions, Inc., Columbia, South Carolina

Brian H. Mason
Langley Research Center, Hampton, Virginia

March 2005

The NASA STI Program Office . . . in Profile

Since its founding, NASA has been dedicated to the advancement of aeronautics and space science. The NASA Scientific and Technical Information (STI) Program Office plays a key part in helping NASA maintain this important role.

The NASA STI Program Office is operated by Langley Research Center, the lead center for NASA's scientific and technical information. The NASA STI Program Office provides access to the NASA STI Database, the largest collection of aeronautical and space science STI in the world. The Program Office is also NASA's institutional mechanism for disseminating the results of its research and development activities. These results are published by NASA in the NASA STI Report Series, which includes the following report types:

- TECHNICAL PUBLICATION. Reports of completed research or a major significant phase of research that present the results of NASA programs and include extensive data or theoretical analysis. Includes compilations of significant scientific and technical data and information deemed to be of continuing reference value. NASA counterpart of peer-reviewed formal professional papers, but having less stringent limitations on manuscript length and extent of graphic presentations.

- TECHNICAL MEMORANDUM. Scientific and technical findings that are preliminary or of specialized interest, e.g., quick release reports, working papers, and bibliographies that contain minimal annotation. Does not contain extensive analysis.

- CONTRACTOR REPORT. Scientific and technical findings by NASA-sponsored contractors and grantees.

- CONFERENCE PUBLICATION. Collected papers from scientific and technical conferences, symposia, seminars, or other meetings sponsored or co-sponsored by NASA.

- SPECIAL PUBLICATION. Scientific, technical, or historical information from NASA programs, projects, and missions, often concerned with subjects having substantial public interest.

- TECHNICAL TRANSLATION. English-language translations of foreign scientific and technical material pertinent to NASA's mission.

Specialized services that complement the STI Program Office's diverse offerings include creating custom thesauri, building customized databases, organizing and publishing research results ... even providing videos.

For more information about the NASA STI Program Office, see the following:

- Access the NASA STI Program Home Page at ***http://www.sti.nasa.gov***

- E-mail your question via the Internet to help@sti.nasa.gov

- Fax your question to the NASA STI Help Desk at (301) 621-0134

- Phone the NASA STI Help Desk at (301) 621-0390

- Write to:
  NASA STI Help Desk
  NASA Center for AeroSpace Information
  7121 Standard Drive
  Hanover, MD 21076-1320

NASA/TM-2005-213525

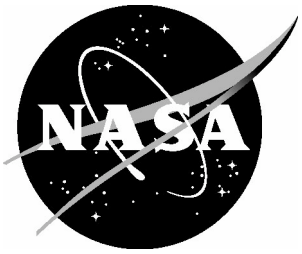

X-43A Rudder Spindle Fatigue Life Estimate and Testing

Edward H. Glaessgen
Langley Research Center, Hampton, Virginia

David S. Dawicke
Analytical Services and Materials, Inc.
Langley Research Center, Hampton, Virginia

William M. Johnston
Lockheed Martin Engineering and Sciences
Langley Research Center, Hampton, Virginia

Mark A. James
National Institute of Aerospace
Langley Research Center, Hampton, Virginia

Micah Simonsen
Correlated Solutions, Inc., Columbia, South Carolina

Brian H. Mason
Langley Research Center, Hampton, Virginia

National Aeronautics and
Space Administration

Langley Research Center
Hampton, Virginia 23681-2199

March 2005

Available from:

NASA Center for AeroSpace Information (CASI)
7121 Standard Drive
Hanover, MD 21076-1320
(301) 621-0390

National Technical Information Service (NTIS)
5285 Port Royal Road
Springfield, VA 22161-2171
(703) 605-6000

Abstract

Fatigue life analyses were performed using a standard strain-life approach and a linear cumulative damage parameter to assess the effect of a single accidental overload on the fatigue life of the Haynes 230 nickel-base superalloy X-43A rudder spindle. Because of a limited amount of information available about the Haynes 230 material, a series of tests were conducted to replicate the overload and in-service conditions for the spindle and corroborate the analysis. Both the analytical and experimental results suggest that the spindle will survive the anticipated flight loads.

Nomenclature

b	=	fatigue strength exponent
c	=	fatigue ductility exponent
E	=	elastic modulus (assumed to be isotropic)
K_b	=	notch sensitivity factor
K_I	=	mode I stress intensity factor
K_{IC}	=	mode I fracture toughness
K_t	=	stress concentration factor
N	=	number of cycles
N_f	=	number of cycles to failure
R	=	fatigue stress ratio (also, fillet radius)
RT	=	room temperature
$\Delta\varepsilon_a$	=	cyclic strain amplitude
ε_f'	=	fatigue ductility coefficient
ε_i	=	Principal strain (i=1,2,3)
ε_{ij}	=	strain (i,j=1,2,3)
σ_{eff}	=	von Mises equivalent stress
σ_f'	=	fatigue strength coefficient
σ_i	=	Principal stress (i=1,2,3)
σ_m	=	mean effective stress
σ_u	=	ultimate stress
σ_{ys}	=	yield stress
τ_{ij}	=	shear stress (i,j=1,2,3)

Introduction

In the summer of 2004, during preparations for flight of the X-43A, one of the rudders on the vehicle was unintentionally overloaded. The X-43A, an unmanned flight test vehicle that will make a single hypersonic flight in late 2004, is shown in Figure 1. Previous finite element analysis determined that the highest stresses and strains during the overload existed at an O-ring groove in the rudder spindle, as shown in Figure 2 [1]. At the request of the X-43A Program Office, a combined analytical and experimental assessment was planned and executed to determine whether or not the static overload would result in premature failure of the rudder spindle during flight test.

Although a fatigue crack growth assessment was originally considered, it was discounted because the magnitude of the overload stresses, residual stresses and plastic strains were likely to violate linear elastic fracture mechanics (LEFM) assumptions. Hence, a strain-life approach including mean stress effects [2] was used to assess the remaining life of the rudder spindle. The strain-life approach is based on the assumption that the fatigue life of notched components can be related to the fatigue life of small unnotched specimens subjected to the same strains as the material at the notch root. Because several important items of information were unknown in this analysis, several assumptions were made to facilitate the calculation of the fatigue life. These assumptions had a significant effect on the life predictions.

Additionally, testing was performed to ensure that the assumptions of the strain life analysis provided a conservative margin of safety for the rudder spindle during in-service loading. A test plan (shown in Appendix A) was developed to experimentally simulate the overload condition as well as the fatigue cycles.

This report documents the assumptions used in the analysis, the life analysis methodology and results, the configuration of the test specimens, the test method and the results of the tests.

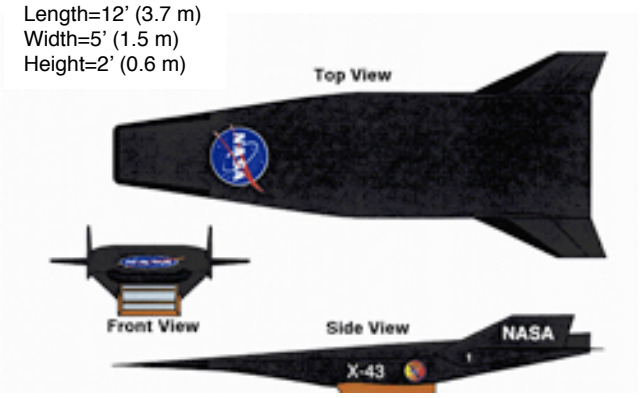

Figure 1. X-43A vehicle

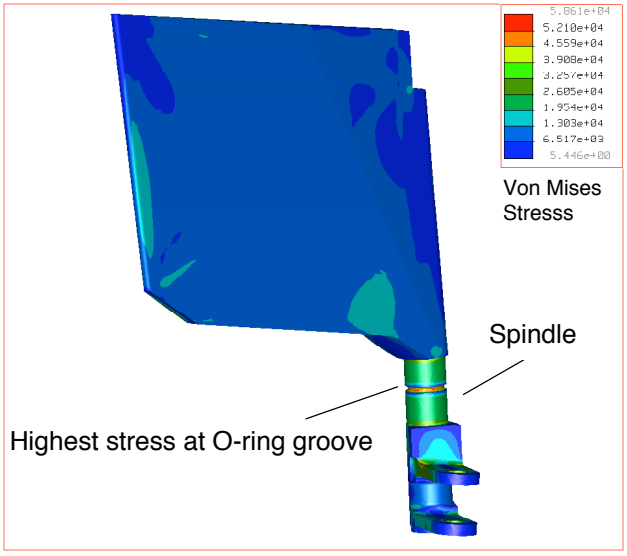

Figure 2. von Mises stress in rudder [1]

Fatigue Life Analysis

Known, Speculative and Assumed Information

This section summarizes the known and speculative information, assumptions made about the material behavior, and assumptions used in the finite element and fatigue life analyses.

Known Information

- The X-43A rudder shaft was inadvertently overloaded to an unknown torque.
- Upon unloading, the rudder had a permanent rotation of approximately 2.5 to 3°.
- The shaft material was Haynes 230 nickel-base superalloy.
- The shaft was hollow with an outside diameter of 0.92 in. and an inside diameter of 0.1875 in.
- The shaft configuration included an O-ring groove with a diameter of 0.8 in. and a fillet (notch) radius of 0.015 in.

Speculative Information

- The O-ring groove was assumed to be the critical location on the rudder shaft after the overload.
- The initial state of the O-ring groove was assumed to be crack and defect free.
- O-ring groove stress levels due to the overload were determined accurately from elastic-plastic finite element analyses [1].
- O-ring groove stress levels due to in-service, cyclic loads were determined accurately from elastic-plastic finite element analyses [1].

• The operational temperature of the shaft is 400°F. This value was the highest measured temperature during a prior test. However, the thermocouple failed before completion of the test, so the actual value is unknown.

Material Assumptions (Data from the Manufacturer [3,4])

• The tensile modulus, yield stress and ultimate stress are: E = 30,600 ksi, σ_{ys} = 56.9 ksi, σ_u = 124.9 ksi, respectively [3].
• The tensile properties reported by the manufacturer, and based on uniaxial testing, were appropriate for modeling cyclic torsional loading.
• The uniaxial strain-life curves that were developed from axial data can be used to accurately predict failure under torsional loading.
• The fracture toughness for mode I loading is: K_{Ic} = 170 ksi $in.^{1/2}$ [4].
• The number of cycles to failure as a function of strain range at zero mean stress for the Haynes 230 alloy at 800°F is shown in Table 1 [3]. (Of the several temperatures for which strain-life curves are provided in [3], 800°F is the closest to the assumed local operating temperature of 400°F.)

Table 1. Haynes 230 data

Total Strain Range (%)	Cycles to Failure
1.5	3,000
1.0	10,000
0.56	100,000

Finite Element Analysis [1] Assumptions†

• Isotropic material hardening is an appropriate constitutive model for Haynes 230 alloy under torsional loading.
• The applied overload torque was 6025 in.-lb. This torque was determined by the analysis as that required to produce a permanent 3° rudder rotation.
• The in-service cyclic torque was ±500 in.-lb., and no other (aerodynamic, bending, etc.) loads were present.

Life Analysis Assumptions

• The stress and strain conditions at the O-ring groove are accurately computed from the finite element analysis as given in Table 2.

Table 2. Stress and strain from finite element analysis [1]

Load Condition	σ_{eff} (ksi)	σ_1 (ksi)	σ_{xx} (ksi)	ε_1
+6025 in.-lb.	94.1	59.3	53.4	0.103
Unload	87.5	54.7	25.9	0.0994
+500 in.-lb.	67.8	46.2	26.9	0.09973
-500 in.-lb.	88.0	57.2	25.0	0.09907

† Finite element analysis provided by Michael Lindell, NASA LaRC [1]

• Linear elastic fracture mechanics (LEFM) assumptions were violated because of the extensive plasticity from overload and peak cyclic stress values local to the O-ring groove. (Thus, LEFM was not used.)
• The strain-life behavior of the shaft was approximated using the data available from tests at 800° F and the data can be extrapolated to failure in one cycle at a strain of 0.4 (40%) at room temperature (RT). This inconsistent extrapolation of data at two different temperatures adds uncertainty, but was necessary to complete the analysis.
• The Coffin-Manson [5] relationship accurately modeled the strain-life behavior of Haynes 230 alloy.
• Mean stress effects on the cyclic loading can be approximated using a mean stress correction to modify the Coffin-Manson relationship [6,7].
• The Palmgren-Miner rule [8,9] for linear cumulative damage was an appropriate tool to account for the damage due to the overload and cyclic loading.
• Load sequence effects are negligible.
• The O-ring groove effects were conservatively accounted for by assuming that the structure was a smooth shaft subjected to the stresses calculated in the finite element analysis.
• Notch sensitivity of the material was unknown and was assumed to be negligible in the overload (6025 in.-lb.) condition. This assumption was not fully substantiated and its consequences could be very significant if even relatively small notch sensitivity exists for Haynes 230 at large plastic strain.
• The fidelity of the finite element mesh was not established [1] and may underestimate the overload strains in the region of high gradient and plastic strain at the filleted region of the O-ring groove. Thus, an additional K_t of 1.5 was included in the overload strains.
• Notch sensitivity was assumed to exist for the Haynes 230 alloy during the in-service (±500 in.-lb.) loading. However, a Neuber notch analysis [2] was not used, because it relies on a parameter that was unknown for this material. Rather, the sensitivity was approximated using a K_b of 5 and is assumed to be a conservative value that also accounts for the unknown fidelity of the finite element mesh in this phase of the analysis.
• Because the material and loading were not well characterized, the NASA STD 5001 safety factor of 4 could not be applied to the fatigue life prediction [10]. A Safety Factor of 10 was used instead.
• All deformation is produced by torsional loading. There were no bending or axial loads in the spindle.

Life Analysis Methodology and Results

This section describes the results of the elastic-plastic finite element analysis [1], the life analysis methodology and results including the Coffin-Manson relationship that was used to relate cyclic strain to fatigue life, and the Palmgren-Miner rule that was used to sum the effects of various damaging cycles. Life predictions based on three different mean stress corrections used to account for the residual stresses that resulted from the overload are also presented.

Elastic-Plastic Stress Strain Behavior Under Torsional Loading
From the elastic-plastic finite element analyses [1]:
Max strain at overload (6025 in.-lb. torque): ε = 0.104
Strain at +500 in.-lb. torque: ε = 0.0997
Strain at –500 in.-lb. torque: ε = 0.09907
Mean effective stress during cyclic loading: σ_m = -77 ksi

Figure 3 illustrates the stress-strain response obtained from the finite element analysis for the finite elements near the base of the O-ring groove during the overload, unload and in-service conditions. The overload torque resulted in a predicted strain of more than 10% and a predicted effective stress of more than 90 ksi at 6025 in.-lb. applied torque. As the applied torque was removed, the region of the O-ring groove initially unloaded elastically from the overload condition and then began to reverse yield as the applied torque reached zero. The in-service -500 in.-lb. torque caused slightly more yielding, and the subsequent ±500 in.-lb. cyclic torque was linear elastic at a high stress ratio with a mean effective stress of -77 ksi.

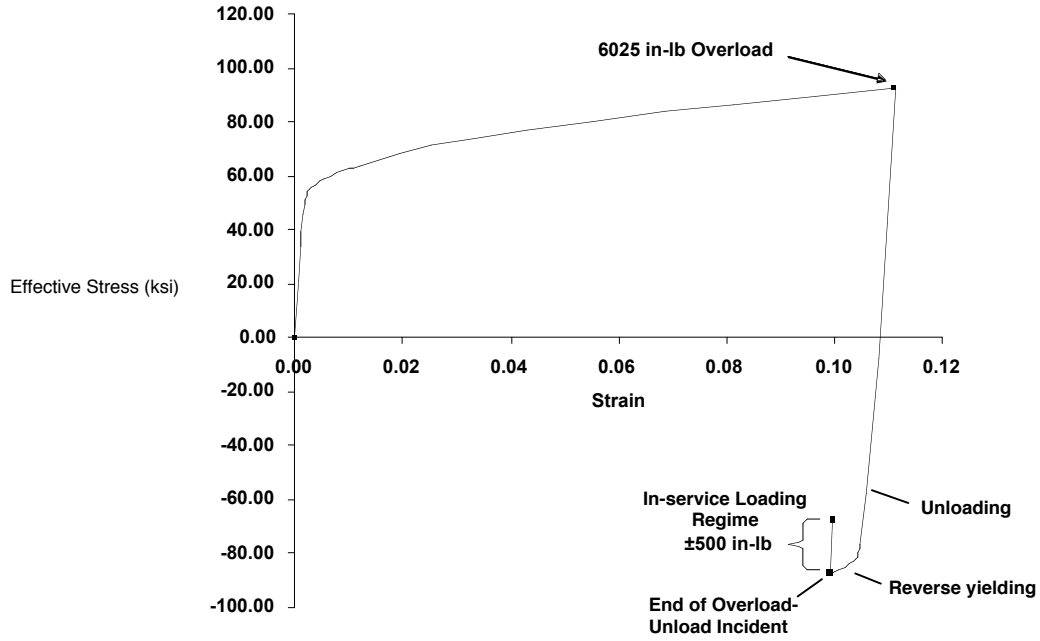

Figure 3. Finite element results for the X-43A rudder overload simulation

Life Analysis Methodology
The relationship between strain and life was determined by fitting the Coffin-Manson [5] relationship in the absence of mean stresses (Eq. 1) to the data† found on p.8 (low cycle fatigue (LCF) curve at 800°F [3]) of the Haynes 230 Alloy material characterization document. Data in reference 3 was available to only 1.5% strain. However, the ultimate strain taken from the uniaxial tensile tests at RT was considered as another data point (1 cycle at 40% strain, see *Life Analysis Assumptions*).

† In general, scatter in fatigue test data is notoriously large. Values for the number of cycles to failure at a given strain range often differ by a factor of two or more. At very low stress levels, factors of 100 are not uncommon [2].

The Coffin-Manson relationship could then be used as

$$\Delta\varepsilon_a = \frac{\sigma_f'}{E}(2N_f)^b + \varepsilon_f'(2N_f)^c \quad (1)$$

with the following values used for the curve fit:
E = 30,600 ksi
σ_f' = 550 ksi
b = -0.12
ε_f' = 0.55
c = -0.48

Because of the residual stresses that resulted from the overload, Eq. 1 was modified using three different mean stress corrections as shown in Eq. 2. Various mean stress corrections are available in the literature (for example, see Refs. 2, 6, 7). Only comparison with test data taken under representative conditions can determine which, if any of the three corrections, is appropriate. In the absence of specific test data, several forms of the mean stress correction are considered:

$$\Delta\varepsilon_a = \frac{\sigma_f'}{E}\left(1-\frac{\sigma_m}{\sigma_f'}\right)(2N_f)^b + \varepsilon_f'\left(1-\frac{\sigma_m}{\sigma_f'}\right)(2N_f)^c \quad \text{(2a, from [6])}$$

$$\Delta\varepsilon_a = \frac{\sigma_f'}{E}\left(1-\frac{\sigma_m}{\sigma_u}\right)(2N_f)^b + \varepsilon_f'(2N_f)^c \quad \text{(2b, from [7])}$$

$$\Delta\varepsilon_a = \frac{\sigma_f'}{E}\left(1-\frac{\sigma_m}{\sigma_u}\right)(2N_f)^b + \varepsilon_f'\left(1-\frac{\sigma_m}{\sigma_u}\right)(2N_f)^c \quad \text{(2c, from [6])}$$

where
σ_u = 124.9 ksi and σ_m = (-)77 ksi.

The ± 500 in.-lb. cyclic strain range was estimated as:

$$K_b(0.0997 - 0.09907) \quad (3)$$

A K_b = 5 was assumed to be more conservative than a typical Neuber approach wherein typical values of K_b at notched shafts are in the range of 2 to 3 [2]. The assumed K_b was used to account for the notch sensitivity during the in-service loading (±500 in.-lb.). Strain values were taken from Ref. 1. Notch sensitivity in the overload condition was assumed to be negligible because of the large plastic strains (see *Life Analysis Assumptions*).

Eqs. 2a, 2b and 2c are shown in graphical form along with the uncorrected Coffin-Manson relationship (Eq. 1) and the available data in Figure 4.

Palmgren-Miner Rule

The Palmgren-Miner rule [8, 9] was used to assess the contributions of the overload cycle and the in-service cycles to the cumulative damage near the O-ring groove:

$$1 = \frac{N_{ol}}{N_{f_{ol}}} + \frac{N_{cy}}{N_{f_{cy}}} \tag{4}$$

where:

N_{ol} = number of applied overload cycles: 1 (at strain ε = 0.104 x 1.5 = 0.156[†])

N_{fol} = number of cycles to failure for the overload strain as calculated by Eq. 2

N_{cy} = number of ± 500 in.-lb. cycles until failure after the overload

N_{fcy} = number of ± 500 in.-lb. cycles until failure if only these cycles were applied, as calculated by Eq. 2.

Life Predictions from Three Mean Stress Corrections

The lives predicted by Eqs. 2a, 2b, and 2c are shown in Table 3. The headings N_{fol}, N_{fcy}, N_{cy} and N_{cy}[‡] represent the number of cycles to failure for the overload condition (6025 in.-lb.) alone, the number of cycles to failure for the in-service condition (±500 in.-lb.) alone, the number of cycles to failure for the in-service condition after a single overload cycle, and the number of cycles to failure for the in-service condition after a single overload cycle and using the Safety Factor of 10, respectively.

Table 3. Life predictions

Model (Eq.)	N_{fol}	N_{fcy}	N_{cy}	N_{cy}[‡]
2a	6	900,000	750,000	75,000
2b	5	100,000	80,000	8,000
2c	1	22,000	0	0

Life predictions using the first two modifications to the Coffin-Manson relationship (Eqs. 2a and 2b) suggest that the spindle would survive the in-service loading requirements, while the third modification (Eq. 2c) suggests that the spindle should not have survived the overload condition. *Clearly, the greatest risk is presented in the uncertainty in the value of N_{fol}.* If this value is less than 2 (i.e., structure would fail prior to completion of a second overload) then it cannot be shown that the vehicle is safe to fly.

[†] Including strain from [1] and factor of 1.5 for unconfirmed fidelity of the finite element mesh

[‡] After applying a safety factor of 10

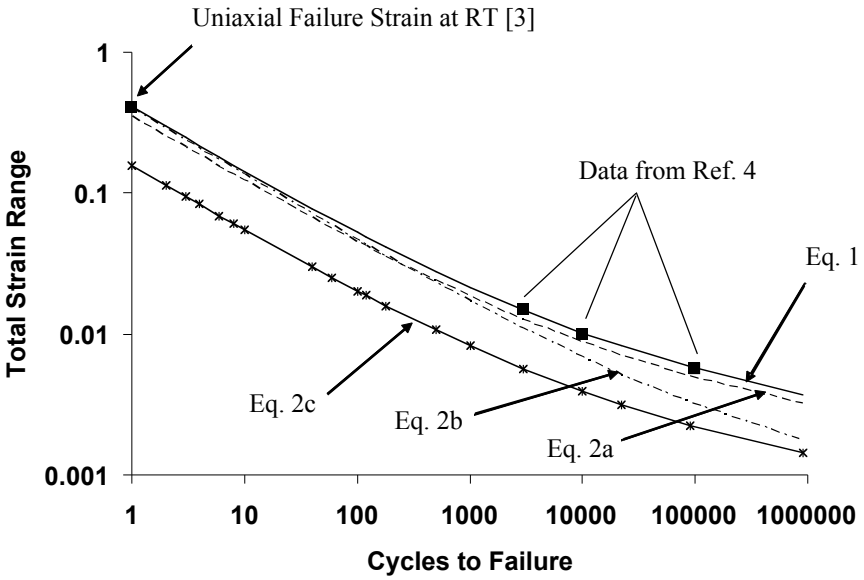

Figure 4. Strain-life curves for Haynes 230 at 800° F and curve fits

Discussion of Fatigue Life Analysis Results

A strain-life analysis was performed using the limited available information on the Haynes 230 material, finite element analysis results [1], a Coffin-Manson relationship to define strain-life behavior in conjunction with several forms of the mean stress correction to account for the residual stress and a Palmgren-Miner rule for linear cumulative damage. Because of a general lack of available information (see *Known, Speculative and Assumed Information*), several conservative assumptions were included in the analysis.

Perhaps the most significant of the assumptions was related to the ability to approximate the effect of the large residual stresses in the vicinity of the O-ring groove. Three forms of the mean stress correction were considered to obtain an assessment of the sensitivity of the predicted life to this contribution to the stress state. Values of 75000, 8000 and 0 cycles were obtained for the corrections shown in Eqs. 2a, 2b and 2c, respectively. It is readily apparent that Eq. 2c is overly conservative at high cyclic strains, since this relationship predicts failure during the overload cycle. However, the results of Eq. 2c were included to demonstrate the sensitivity of the results to the mean stress approximation.

Although the recommendations were not determined specifically for Haynes 230, Ref. 7 suggests that in low cycle fatigue, with large cyclic plastic strain, the mean stress effects on total life can be ignored, resulting in the curve shown for Eq. 2b in Figure 4. Note that this curve agrees with the uncorrected results (Eq. 1) for high cyclic strain and accounts for the mean stress effect at low cyclic strain similar to Eq. 2c. Although the reasoning presented here was *not validated*, this argument gives some credence to the suggestion that Eq. 2b, giving a remaining life of 8000 cycles, was conservatively representative of the behavior of the rudder spindle.

Experimental Program

The fatigue life analysis was based on a number of assumptions including the extrapolation of strain-life data. Because of the unknown fidelity of the assumptions required in the analysis, a series of simple torsion tests was conducted to corroborate the fatigue life assessment and to ensure that the specimen did not fail in a predetermined lifetime. A specimen was designed that approximated the O-ring groove and could be tested in existing servo-hydraulic equipment. The tests consisted of two sequential loading conditions, including a static overload to impart permanent deformation and fatigue cycling to simulate flight conditions.

Test Specimens

Four specimens were fabricated in accordance with the drawings shown in Figure 5. The specimen length and reduced dimension near the ends were required by the experimental set up. The remainder of the dimensions including specimen diameter and O-ring groove configuration are the same as in the X-43A rudder spindle. An additional test article, termed the *blank* in this report, was manufactured with the same dimensions as the specimens, but without the O-ring groove, and was used to tune the load frame and refine the test procedure. The specimens were machined from a single billet of Haynes 230 nickel-base superalloy and were inspected for manufacturing defects before testing [11].

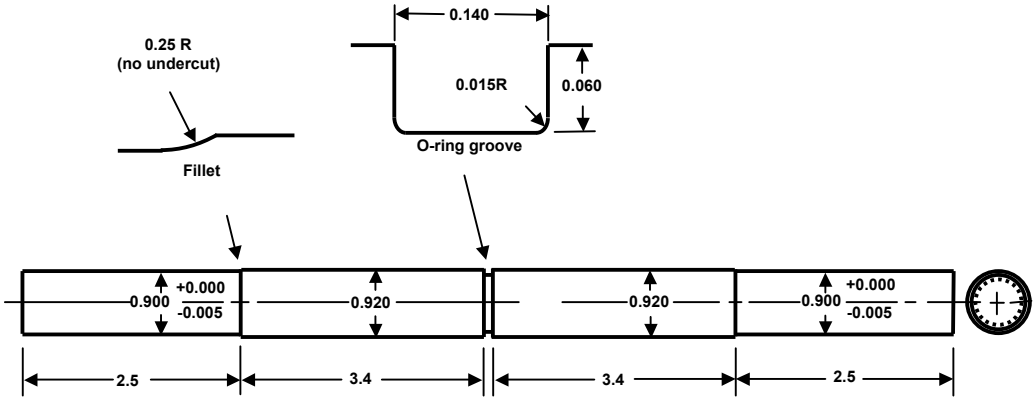

Note: All dimensions in inches

Figure 5. Test specimen

A length of approximately 2” at each end of the specimens was held by the hydraulic grips during the overload, and a length of approximately 1” at each end of the specimens was held by the hydraulic grips during the fatigue loading. The shorter gripping length during the fatigue tests was needed to allow room for the oven and water jackets used to simulate in-service temperature conditions and was possible because of the significantly lower torque applied during the fatigue tests.

Test Method

Static overload testing at room temperature and cyclic fatigue testing at elevated temperature were conducted as part of this incident investigation. The specimens were tested in a servo-hydraulic tension-torsion load frame at NASA LaRC. The load frame, shown in Figure 6, has a capacity of 20 kips axial load and 10,000 in.-lb. torque.

Test Matrix

The test matrix for the specimens is shown in Table 4. Since the values of the permanent rotation of the X-43A rudder spindle were not precisely known (estimates ranged from 2.5° to 3.0°) a target value of 3.0° was chosen for specimen 1. To be conservative, slightly higher target values were chosen for specimens 2 and 3. The overload was performed monotonically, under angular displacement control and at room temperature (RT). Then, each specimen was tested in fully reversed cyclic loading (R=-1) at ±500 in.-lb. for 5000 cycles. Five thousand cycles was 2 orders of magnitude greater than the expected life of the spindle and was defined as "run-out." Specimens 1 and 2 were tested at 400°F, while specimen 3 was tested at 800°F. Note that specimen 4 was held in reserve and ultimately was not tested.

Table 4. Test matrix

Specimen	Target Rotation for Overload (°)	Temperature During Overload	Cyclic Fatigue Torque (in.-lb.)	Number of Fatigue Cycles	Temperature During Fatigue (°F)
1	3.00	RT	±500	5000	400
2	3.25	RT	±500	5000	400
3	3.50	RT	±500	5000	800
4	Not tested	-	-	-	-

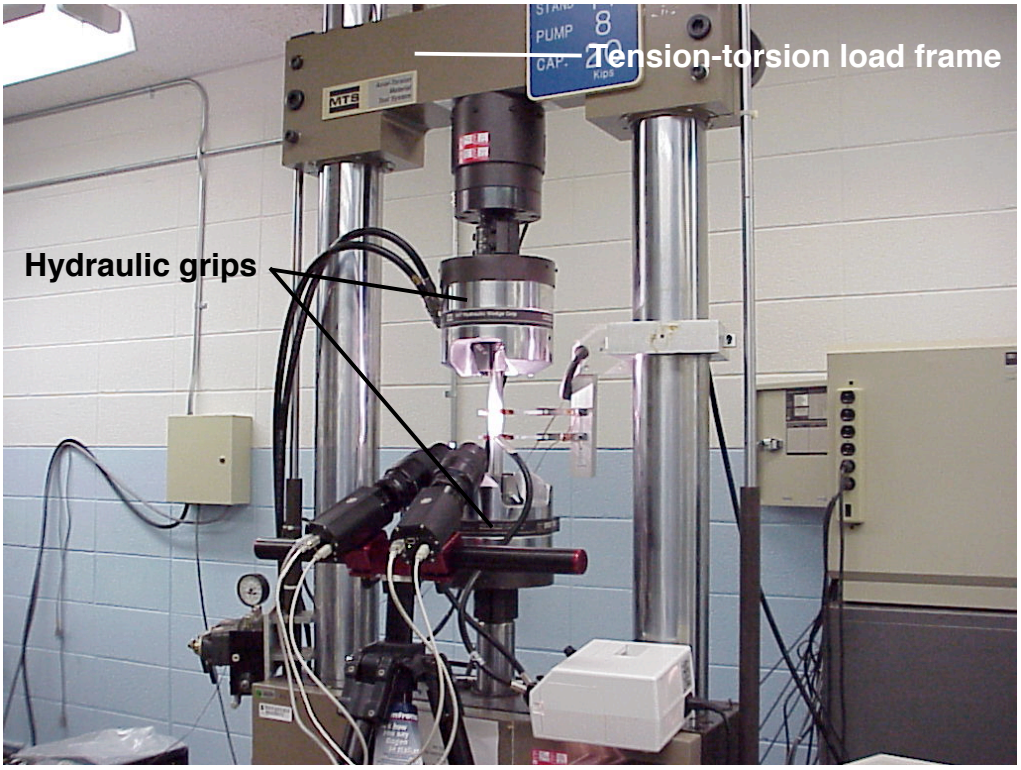

Figure 6. Tension-torsion load frame

Static Overload Testing

The specimen was loaded in angular displacement (rotation) control at a rate of 0.02 degrees/second. Additionally, the control system translated the actuator vertically as needed to prevent an axial force in excess of approximately ±10 lb. from being induced due to the rotational deformation.

Although the original finite element analysis [1] did not predict yielding of the net section, preliminary testing of the un-notched *blank* to the load assumed in the analysis (6025 in.-lb.) revealed that net section yielding occurred and resulted in approximately 5° of permanent offset over the length of the *blank*. The implication of net section yielding is that all of the plastic deformation does not occur at the O-ring groove as was predicted by the finite element analysis. Thus, a gage section of 1.5", corresponding to the approximate length of the X-43A rudder spindle, was defined. A local relative rotation was *estimated* by monitoring the rotations at approximately 0.75" above and 0.75" below the center of the O-ring groove using the relative rotation measurement apparatus (RRMA) shown in Figure 7. The rotations were monitored during the test by mounting "fingers" to the specimen immediately above and below the gage section as shown in Figure 8. As the region above and below the gage section rotated, the fingers contacted and loaded cantilevered strips of spring steel causing a strain to be measured by each of two uniaxial strain gages (shown in Figure 8). Each of the strains was then correlated to the rotation of the corresponding "finger". Thus, by monitoring the two values of strain

during the test, a relative rotation across the gage section could be estimated. This relative rotation became the revised metric for angular deformation of the spindle.

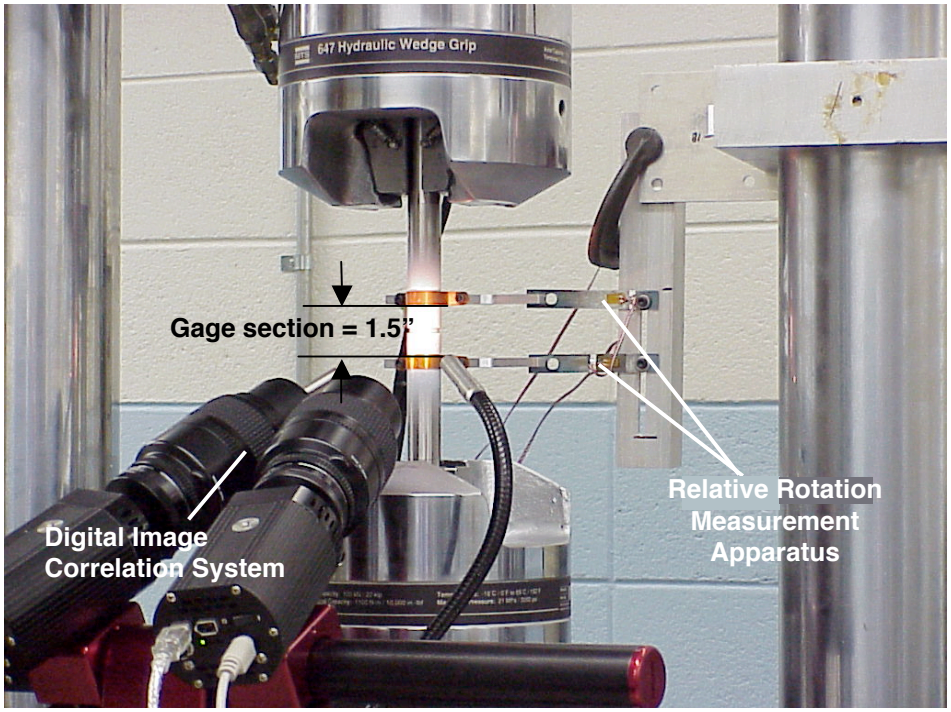

Figure 7. Digital image correlation system and relative rotation measurement apparatus

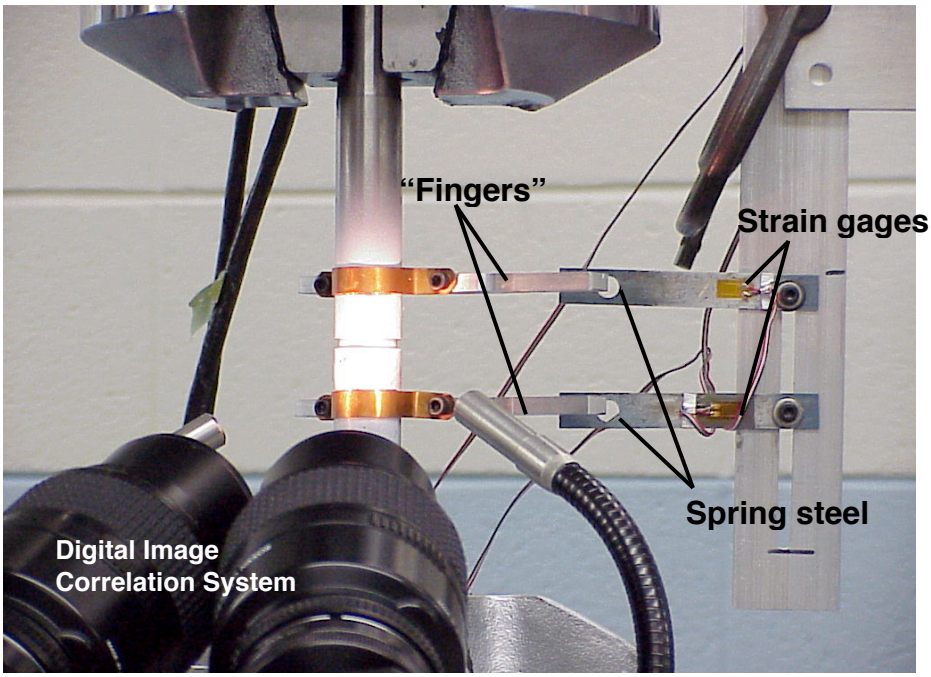

Figure 8. Detail of imaging system and relative rotation measurement apparatus

Note that the relative rotation measurement taken during the test included both an unrecoverable (plastic) component and a recoverable (elastic) component. The elastic component was estimated and added to the desired plastic component to determine the target relative rotation during the test. After the specimen was unloaded, only a residual plastic component remained. Although this method was expected to provide reasonable relative rotation measurements during the test, the final measurements of the permanent rotation were determined by marking scribe lines axially on the specimen before and after testing, allowing a more precise measurement of permanent deformation after the test.

Digital Image Correlation

Real-time measurement of the three-dimensional deformation and strain fields in the vicinity of the O-ring groove for each of three specimens was performed [12]. Each specimen was prepared by, first, cleaning the area near the O-ring groove, then, coating the area with white paint, and finally, applying a speckle pattern over the painted area. The speckle pattern was produced by blowing toner powder over the painted area. Two digital cameras, fitted with 105mm lenses, were used to image the specimen as shown in Figures 7 and 8. Lighting was provided by a dual head fiber optic illuminator. The local displacement field on the surface of the spindle was determined by monitoring the displacement of small regions of the "speckled patterns." Images were taken every 10 seconds or approximately every 0.20 degrees of relative rotation.

Images were taken from the two cameras so that a three-dimensional displacement field could be measured and the corresponding strain field could be derived. An automated system [12] was used to reduce the image data to strain and displacement fields. A sample of the image pairs, from each of the two cameras, is shown in Figure 9. For each specimen, displacement fields were calculated for every 0.20° of relative rotation.

The local strains were calculated by differentiating the displacement field in 31x31 point windows. This imaging approach resulted in a total equivalent gage size of 62 pixels or approximately 0.013" [12].

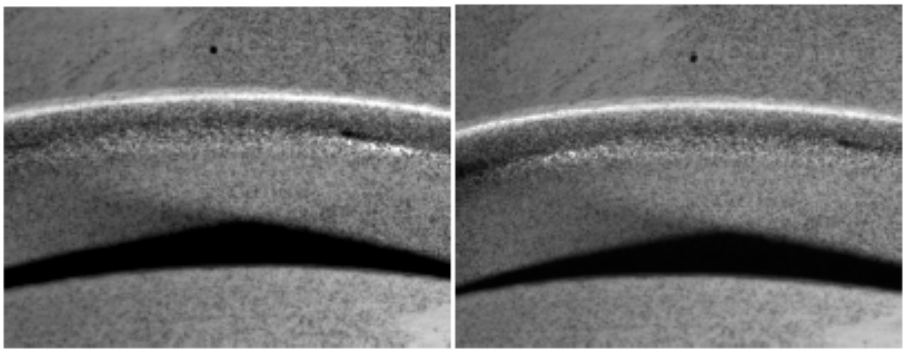

Figure 9. Image pair

Cyclic Fatigue Testing

After overloading each of the specimens at room temperature, preparations for cyclic fatigue testing at elevated temperature (400°F and 800°F) began. Because the maximum operational temperature of the wedge grips was only 150°F, a means of cooling the portion of the test specimen that extended into the grips was needed. A water jacket was fashioned by coiling copper tubing around the specimen and attaching the lines to a water supply. To ensure that the target temperature was reached in the vicinity of the O-ring groove, thermocouples were mounted to the specimen near the top and bottom of the gage section. Additionally, thermocouples were spot welded to the wedge grips near the interface with the specimen to monitor wedge grip temperature. The temperature in the gage section was maintained to within 10°F of the target (400°F or 800°F) temperature. The fatigue tests were not begun until the specimens reached and maintained their target temperature for approximately 15 minutes. Details of the oven, water jackets and thermocouple placement are shown in Figure 10. Note that the digital image correlation system could not be used for the fatigue tests because the oven prevented accessibility to the gage section.

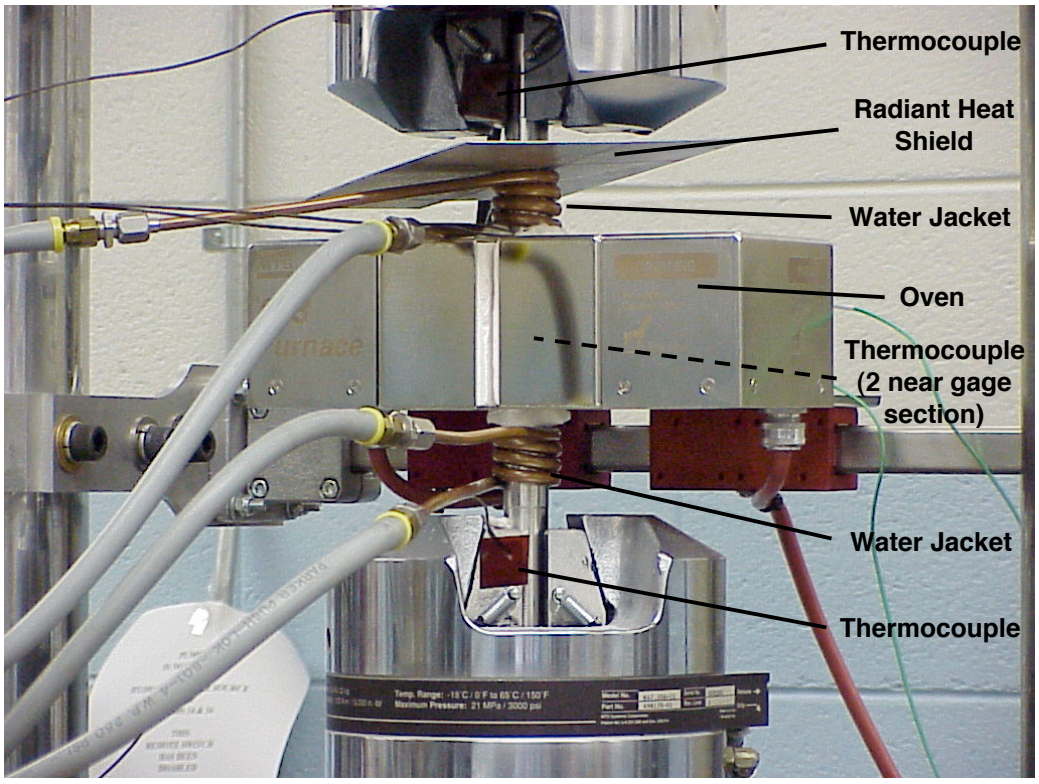

Figure 10. Oven and water jacket

Non-Destructive Evaluation (NDE)

NDE was performed by the specimen manufacturer (ATK) on all test specimens before they were shipped to LaRC. Additionally, NDE was performed at LaRC using visible

dye penetrant according to LaRC LMS-TD-5561 and following the schedule shown in Table 5. See Appendix B for the inspection report.

Table 5. NDE schedule

Specimen	As Received	After Overload	25 cycles	100 cycles	500 cycles	1000 cycles	5000 cycles
1	☒	☒	☒	☒	☒	☒	☒
2	☒	☒				☒	☒
3	☒	☒				☒	☒
4*	☒						

☒ NDE performed
* Not tested

Discussion of Experimental Results

Displacements

The torque-rotation response of the 1.50" gage section generated for specimens 1, 2 and 3 using the RRMA are shown in Figure 11. The response in the linear loading portion of the torque-rotation curve was nearly identical for all three specimens and only minor differences were seen in the nonlinear loading portion of the curve. Additionally, the slope of the unloading portion of the curves were nearly identical for all three specimens and was nearly the same as for the linear loading portion of the curves. Only a minor indication of reverse yielding is seen near the lower portion of the unloading curves.

Figures 12 and 13 show the torque-rotation and torque-opening displacement curves, respectively, across the O-ring groove of specimen 3 measured using the digital image correlation system. These values are the localized deformation determined as the difference in the measured displacements immediately adjacent to either side of the 0.140" wide O-ring groove. The torque-rotation measurements across the O-ring groove were necessarily smaller than the values measured across the 1.50" gage section determined using the RRMA. Also, the torque-opening displacement values shown in Figure 13 did not exceed 0.001 inches (0.022 mm) at any point in the loading cycle. The scatter in the values of measured torque as a function of opening displacement indicates that the magnitude of opening displacement was near the limit of the resolution of the imaging system.

The permanent rotation target value; measured rotation determined using the RRMA, scribe marks, and digital image correlation system; and the O-ring groove opening displacement determined using calipers and the digital image correlation system are given in Table 6. All of these displacement values were determined after the specimen was unloaded. The measured rotation taken from the RRMA and the scribe lines were in reasonable agreement indicating that the curves in Figure 11 were representative of the torque-rotation response of the gage section. Again, the local rotation at the O-ring groove measured using the digital image correlation system was somewhat smaller than the gage section rotation indicating that some yielding does occur away from the O-ring

groove. Also, the digital image correlation system shows a change in O-ring groove opening dimension of 8.5E-4 inches whereas the resolution of the calipers was not sufficient to show this small change.

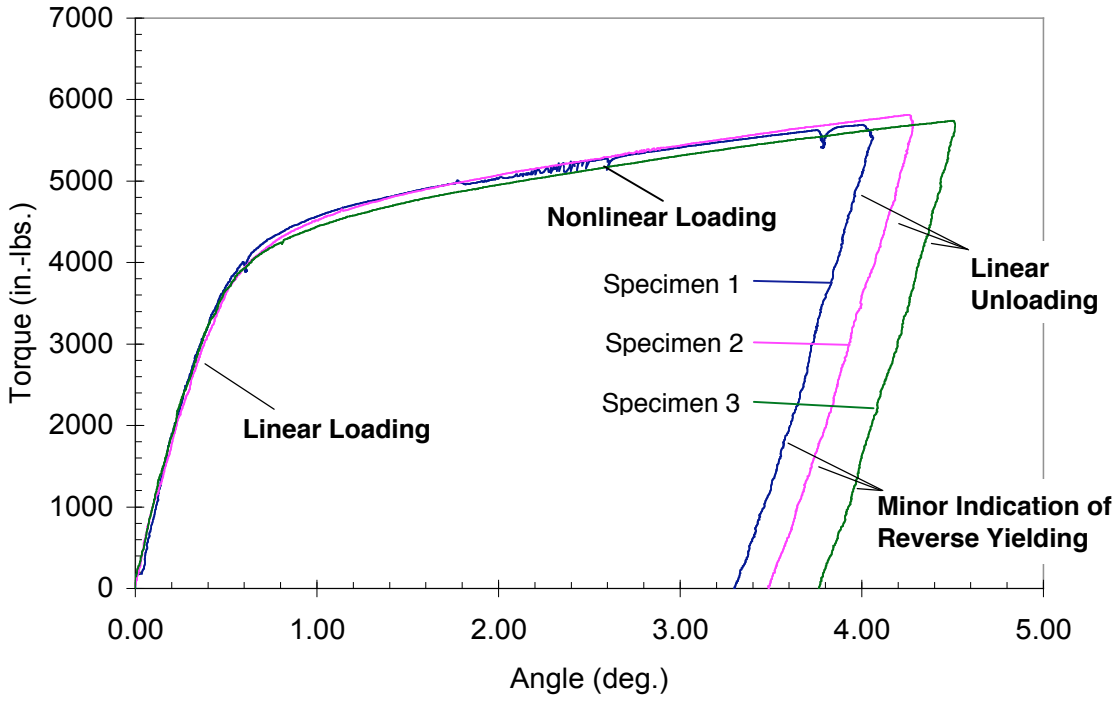

Figure 11. Gage section torque-rotation curves from RRMA

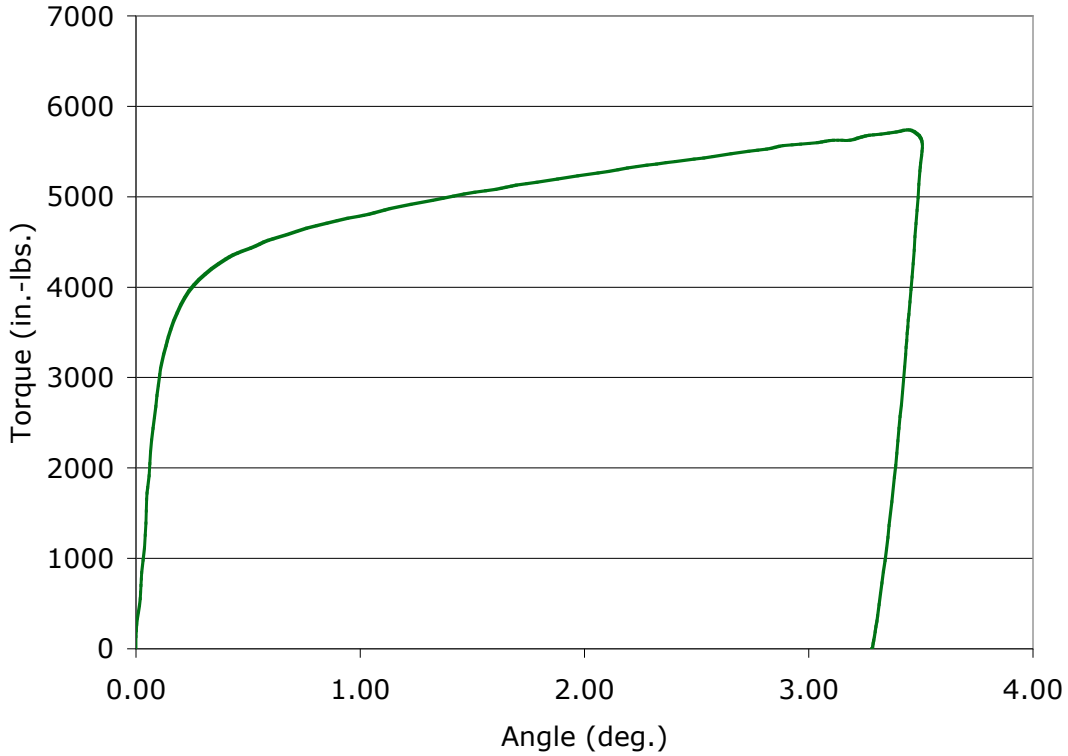

Figure 12. O-ring groove torque-rotation curve for Specimen 3 from the digital image correlation system

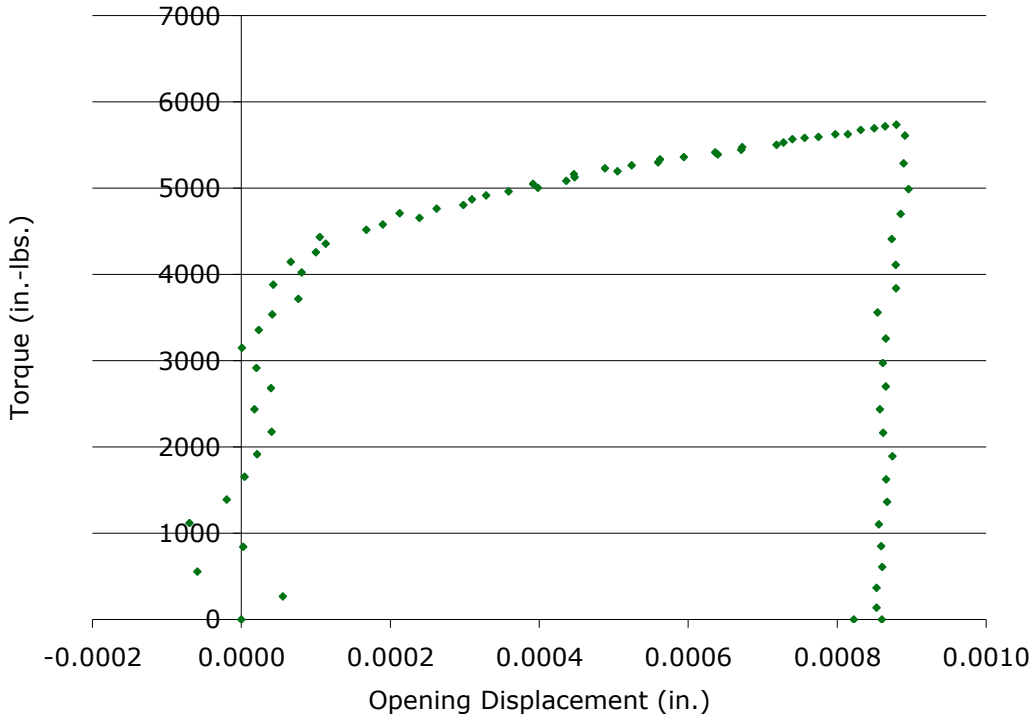

Figure 13. O-ring groove torque-opening displacement curve for Specimen 3 from the digital image correlation system

Table 6. Permanent deformation after overload

Specimen	Target Rotation (°)	Measured Rotation (RRMA) (°)	Measured Rotation (Scribe) (°)	Measured Rotation (Digital Image) (°)	Goove Opening Displ. (Caliper) (in.)	Goove Opening Displ. (Digital Image) (in.)
1	3.00	3.29	2.85	-	0.000	-
2	3.25	3.48	3.21	-	0.000	-
3	3.50	3.74	3.60	3.28	0.000	8.5E-4
4	Not tested	-	-	-	-	-

Displacement and Strain Fields

The digital image correlation system was used to obtain three-dimensional displacement and strain fields during the overloading of specimens 1, 2 and 3. For brevity, only specimen 3 will be discussed further. The total shear strain field in the vicinity of the O-ring groove of specimen 3 at the maximum torque (5737 in.-lb.) was measured with a peak strain of 13.6%, as shown in Figure 14. Note that this value is much larger (13.6% strain at 5737 in.-lb. torque) than the value predicted by the finite element analysis (10.4% strain at 6025 in.-lb. torque). The residual permanent (plastic) shear strain at zero torque in the same region of specimen 3 was measured with a peak strain of 13.4%, as

shown in Figure 15. Although the contours were determined at only a small region of the O-ring groove, the shear strain fields are assumed to be axisymmetric.

Note that the maximum shear strain in Figures 14 and 15 occurs along the flat portion of the O-ring groove near the 0.015" radius. Because of the symmetry of the specimen, a similar strain field is assumed to exist near the other 0.015" radius.

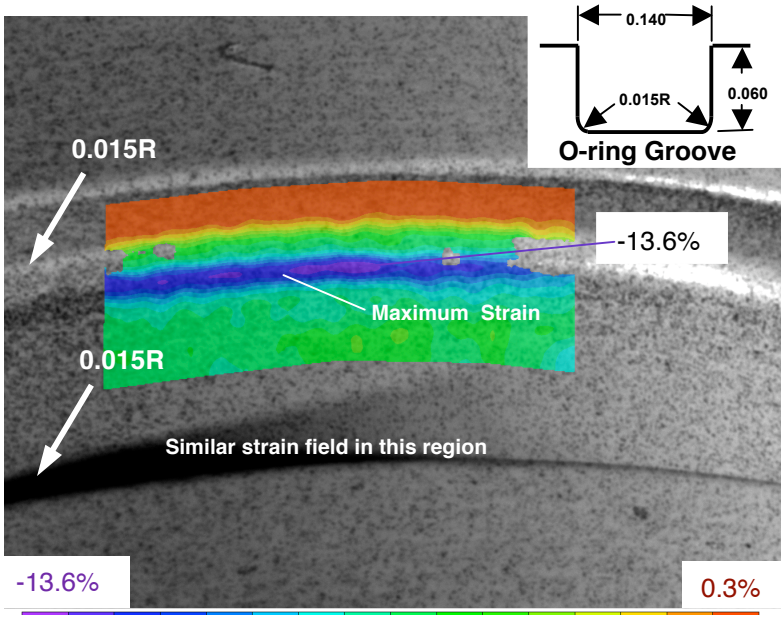

Figure 14. Total shear strain at maximum torque near O-ring groove of specimen 3

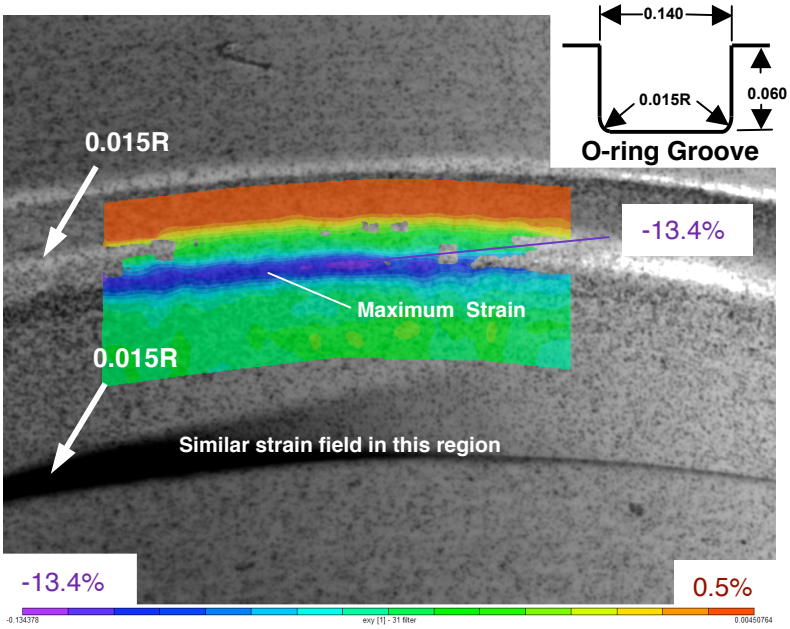

Figure 15. Residual permanent (plastic) shear strain near O-ring groove of specimen 3

Detection of Cracks

Specimens 1, 2 and 3 survived 5000 cycles of ±500 in.-lb. applied torque at 400°F, 400°F and 800°F, respectively. Note that specimen 3 was tested at 800°F because the thermocouple that was used (during a prior test) to establish the in-service temperature failed at 400°F, leaving some uncertainty about the in-service value. As shown in Table 7, no cracks were found in specimens 1 and 2 using visual techniques. However, a small (0.004") possible longitudinal crack was found near one of the 0.015" radii of the O-ring groove in specimen 3 after 5000 cycles. This feature could not be verified without destructive examination of the specimen. Such verification was deemed unnecessary because the goal of the testing was to confirm the ability of the rudder spindle to survive 5000 in-service cycles, thus, any damage state that did not prevent the rudder from carrying ±500 in.-lb. torque was irrelevant.

Table 7. Detection of Cracks

Specimen	Test Temp. (°F)	As Received	After Overload	25 cycles	100 cycles	500 cycles	1000 cycles	5000 cycles
1	400	None	None	None	None	None	None	None
2	400	None	None	-	-	-	None	None
3	800	None	None	-	-	-	None	1x0.004"
4	Not tested	-	-	-	-	-	-	-

Concluding Remarks

At the request of the X-43A program office, a combined analytical and experimental assessment was planned and executed to determine whether or not a static overload (corresponding to a measured 3° permanent offset) would result in premature failure of the rudder spindle during flight test.

The fatigue life analysis used the very limited available test data with a Coffin-Manson relationship and three different mean stress corrections to relate cyclic strain to fatigue life, and the Palmgren-Miner rule to sum the effects of the various damaging cycles. The assessment was shown to be highly dependent on the assumed mean stress correction used to account for the residual stresses that resulted from the overload. Further, the notch sensitivity of the Haynes 230 material was unknown, and the limited cyclic fatigue data and ultimate stress data were developed at different temperatures. Although the life assessment suggested that the overload condition did not preclude use of the existing spindle, because of the many assumptions required for the analysis, prudence dictated that the analysis be corroborated by the testing of a representative configuration at conditions similar to those experienced by the spindle.

Thus, an experimental program was planned and executed to corroborate the analytical fatigue life assessment. Four specimens, that mimicked the configuration of the rudder

spindle as closely as possible, were manufactured. Because the precise amount of permanent rotation was not known, three target values of overload rotation were considered and corresponded to 3.00°, 3.25° and 3.50°. Deformation of the test specimens was determined across a 1.5" gage length corresponding to the length of the rudder spindle, and locally, across the 0.140" wide O-ring groove. Additionally, strain values were measured at the O-ring groove using the digital image correlation system. The specimens were then cyclically loaded to ±500 in.-lb. torque for 5000 cycles. Because the in-service temperature was not precisely known, two specimens were tested at 400°F, while a third was tested at 800°F. All specimens survived the cyclic loading after surviving their respective overload cycle.

While no amount of analysis or testing can guarantee that the previously overloaded X-43A rudder spindle would survive its in-service loading, the program that is described in this report is believed to be as rigorous as possible, considering the lack of information about the material and the in-service and overload conditions. In the many instances where information was unavailable or believed to be speculative, an attempt was made to make estimates that were slightly conservative. Despite the many conservative assumptions in both the analysis and testing, the X-43A rudder spindle was shown to be safe for flight.

Acknowledgements

The authors wish to thank Steve Lee, David Barnes and Ed Townsley of the Applied Technologies and Testing Branch at NASA LaRC for facilitating the test set-up and operating the laboratory equipment during testing. Additional thanks are due C.H. Greenhalgh of the Quality Applications Technology Branch for performing the non-destructive evaluation of the test specimens. Many helpful conversations with Dwaine Klarstrom of Haynes International and Steve Hales of the Metals and Thermal Structures Branch of NASA LaRC are acknowledged.

References

1. Michael Lindell, "Hyper-X Mach 10 Vehicle, Analysis of Rudder and Wing Loads Due to Contact Incident," Presentation Viewgraphs, July 8, 2004.
2. H.O. Fuchs and R.I. Stephens, *Metal Fatigue in Engineering*, John Wiley & Sons, Inc., 1980, Chapters 5-8.
3. "Haynes 2003 Alloy," http://www.haynesintl.com/pdf/h3000.pdf.
4. Dwaine Klarstrom, Haynes International, Private Communication, Aug 6, 2004.
5. L.F. Coffin, "The Flow and Fracture of a Brittle Material," *Journal of Applied Mechanics*, Vol. 17, Sept. 1950, pp. 233-248.
6. N. E. Dowling, *Mechanical Behavior of Materials*, Prentice-Hall, Inc., 1993, pp. 639-641.
7. D. Fang and A. Berkovits, "Mean Stress Models for Low-Cycle Fatigue of a Nickel-Base Superalloy," *International Journal of Fatigue*, Vol.16, pp. 429-437, 1994.
8. Palmgren, "Durability of Ball Bearings," *ZVDI*, Vol. 68, No. 14, pp. 339-341, 1924.

9. M. A. Miner, "Cumulative Damage in Fatigue," *Journal of Applied Mechanics*, Vol. 12, pp. A159-A164, 1945.
10. NASA Standard 5001: Structural Design and Test Factors of Safety for Spaceflight Hardware, Section 5.2: Fatigue and Creep, June 1996.
11. Risner, Noah, Assorted ATK Manufacturing and Quality Assurance Information – Shipped with Test Specimens, September 1, 2004.
12. Simonsen, Micah, "Control Shaft Test Results," Report from Correlated Solutions, Columbia, SC, http://www.correlatedsolutions.com, September 27, 2004.

Appendix A: X-43A Spindle Test Plan

Background

Four torsion tests will be conducted on a cylindrical spindle with O-ring grooves and made from Haynes 230 material. The tests will attempt to simulate the torsional overload experienced by the X-43A rudder shaft and confirm the number of operational cycles that the shaft can experience before failure.

Specimen Design and Testing

Four specimens will be manufactured from the Haynes 230 material used in the X-43A rudder shaft. A fifth specimen (the blank) made from Haynes 230 but not having the O-ring groove will be used to tune the load frame. The specimen design is shown in Figure A1.

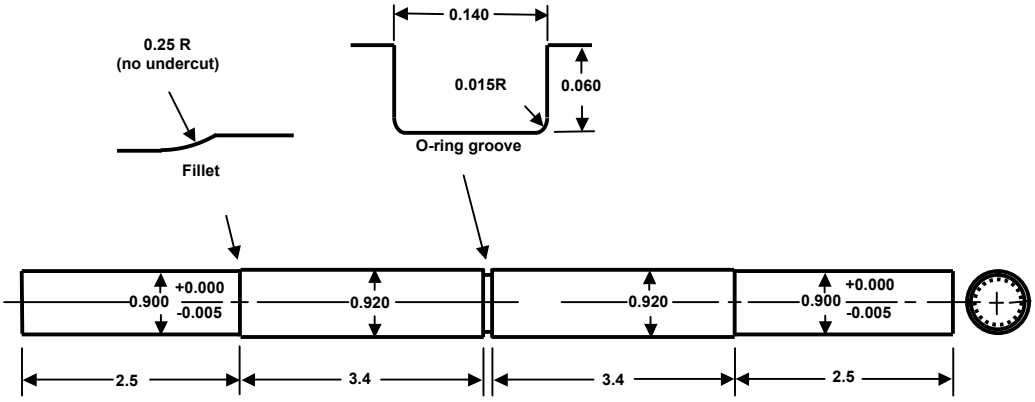

Note: All dimensions in inches

Figure A1. Test specimen

Measurement Techniques

- Measurements of rotational displacement will be obtained from the load frame controller output. Measurements will be made during the overload, unloading and fatigue cycles.
- A 3-dimesional digital image correlation system will be used to obtain strain and displacement measurements in a 5mm x 5mm area around the notch root during the overload and unloading only.

Test Equipment

- A tension/torsion load frame located at LaRC in B1205 with a capacity of 10,000 in.-lbs. will be used to conduct the tests. The finite element analysis

predicted a torque of 6,025 in.-lbs. would result in a 2.75-degree permanent offset of the shaft, so the capacity of the load frame should be sufficient.

• An attempt will be made to use an oven to heat the specimen during the operational cyclic loading (fatigue loading). The limited size (12 inches) of the available material may make it impossible to utilize the oven because of a lack of space for cooling coils needed to prevent damage to the grips.

• A 3-dimensional digital image correlation system will be utilized to measure strains at the notch.

Test Procedure

A. Machine tuning
   a. Install the blank in the grips
   b. Tune tests stand for the provided specimen stiffness
   c. Conduct the required cyclic and monotonic loading steps to insure proper test stand response

B. Initial overload
   a. Measure O-ring groove dimensions
   b. Perform NDE (dye Penetrant) inspection of O-ring groove
   c. Coat the O-ring notch for digital image correlation measurements
   d. Install first specimen in the grips
   e. Torque to 6025 in.-lbs., unload and measure permanent deformation
      i. Capture digital image correlation images every 1,000 in.-lbs. (loading and unloading)
      ii. Capture digital image correlation images at peak load
      iii. Capture digital image correlation images at unloaded condition
      iv. Measure O-ring groove dimensions
      v. Perform NDE (dye Penetrant) inspection of O-ring groove
   f. Adjust the maximum torque as necessary to obtain 2.75° of permanent deformation for the subsequent specimens.
      i. Capture digital image correlation images every 1000 in.-lbs. (loading and unloading)
      ii. Capture digital image correlation images at peak load
      iii. Capture digital image correlation images at unloaded condition
      iv. Measure O-ring groove dimensions
      v. Perform NDE (dye Penetrant) inspection of O-ring groove

C. Operational cycling[†]
   a. Install specimen in the grips
   b. Attempt to install oven and cooling coils
   c. If oven is used, heat to a temperature to 400° F[‡]
   d. Cycle first specimen from 500 in.-lbs. to –500 in.-lbs. for 25 cycles at 1-5 Hz.
      Perform NDE (dye Penetrate) inspection of O-ring groove
      Continue “d” and perform NDE at 100, 500, 1000 and 5000 cycles, or until failure
   e. Duplicate test with second specimen
   f. If both specimens survive 5000 cycles, then test the 3rd specimen at 1000°F. (Thermocouple readings near the spindle stopped prematurely at 400°F. In the

event that this is an issue, 1000°F gives additional confidence that the specimen will survive in-flight conditions.)

g. If the specimen that is subjected to 1000° F survives 5000 cycles, then cycle the 4th specimen from 0 to 6025 in.-lbs. until failure at room temperature to better understand the effects of the overload cycle on life.

† Modification to items B and C may be made as warranted during the test. Since the primary goal is to reach 2.75° permanent offset at room temperature and cycle at ±500 in.-lb. at 400°F, these conditions will be obtained before other conditions are attempted. It is possible but not likely that iteration using all four specimens will be required to meet the primary goal.

‡ If the oven cannot be used, we will need to consider the effects of temperature on fatigue life and revise our estimation of the number of cycles required to obtain confidence in the durability of the spindle.

Appendix B: NDE Inspection Report Results

A dye penetrant inspection report was provided on 10/4/2004 by C.H. Greenhalgh of the Quality Applications Technology Branch at NASA Langley Research Center. Pertinent information from that report follows:

Penetrant Type: DP-51
Developer Type: D-100
Removal Type/Solvent: Water
Manufacturer: Sherwin, Inc.
Dwell Time: 30 min
Temperature: 72°F

Inspection Code or Requirement: ASME Sect V
NDES Procedure: LMS-TD-5561

Items Inspected:
Item 1.) X-43 Specimen #1. Inspected after 25 cycles on 9/24, 100 and 500 cycles on 9/27, 1000 and 5000 cycles on 9/28.
Item 2.) X-43 Specimen #2. Inspected after 1000 cycles on 9/28 and 5000 cycles on 9/29.
Item 3.) X-43 Specimen #3. Inspected after 1000 cycles on 9/29 and 5000 cycles on 9/30.

Results:
No relevant indications on Specimens 1 and 2. Linear indication, 0.004" in length, on Specimen #3 after 5000 cycles.

Notes:
All items inspected prior to the beginning of testing.

REPORT DOCUMENTATION PAGE

Form Approved
OMB No. 0704-0188

1. REPORT DATE *(DD-MM-YYYY)*	2. REPORT TYPE	3. DATES COVERED *(From - To)*
01- 03 - 2005	Technical Memorandum	

4. TITLE AND SUBTITLE

X-43A Rudder Spindle Fatigue Life Estimate and Testing

5a. CONTRACT NUMBER

5b. GRANT NUMBER

5c. PROGRAM ELEMENT NUMBER

6. AUTHOR(S)

Glaessgen, Edward H.; Dawicke, David S.; Johnston, William M., Jr.; James, Mark A.; Simonsen, Micah; and Mason, Brian H.

5d. PROJECT NUMBER

5e. TASK NUMBER

5f. WORK UNIT NUMBER

23-064-50-10

7. PERFORMING ORGANIZATION NAME(S) AND ADDRESS(ES)

NASA Langley Research Center
Hampton, VA 23681-2199

8. PERFORMING ORGANIZATION REPORT NUMBER

L-19082

9. SPONSORING/MONITORING AGENCY NAME(S) AND ADDRESS(ES)

National Aeronautics and Space Administration
Washington, DC 20546-0001

10. SPONSOR/MONITOR'S ACRONYM(S)

NASA

11. SPONSOR/MONITOR'S REPORT NUMBER(S)

NASA/TM-2005-213525

12. DISTRIBUTION/AVAILABILITY STATEMENT

Unclassified - Unlimited
Subject Category 26
Availability: NASA CASI (301) 621-0390

13. SUPPLEMENTARY NOTES

An electronic version can be found at http://ntrs.nasa.gov

14. ABSTRACT

Fatigue life analyses were performed using a standard strain-life approach and a linear cumulative damage parameter to assess the effect of a single accidental overload on the fatigue life of the Haynes 230 nickel-base superalloy X-43A rudder spindle. Because of a limited amount of information available about the Haynes 230 material, a series of tests were conducted to replicate the overload and in-service conditions for the spindle and corroborate the analysis. Both the analytical and experimental results suggest that the spindle will survive the anticipated flight loads.

15. SUBJECT TERMS

X-43A; Rudder; Spindle; Overload; Fatigue life

16. SECURITY CLASSIFICATION OF:			17. LIMITATION OF ABSTRACT	18. NUMBER OF PAGES	19a. NAME OF RESPONSIBLE PERSON
a. REPORT	b. ABSTRACT	c. THIS PAGE			STI Help Desk (email: help@sti.nasa.gov)
					19b. TELEPHONE NUMBER *(Include area code)*
U	U	U	UU	31	(301) 621-0390